Infrared diode laser spectroscopy of O_2–N_2O van der Waals complex in the ν_1 symmetric stretch region of N_2O*

Li Song(李 松)[a)b)], Zheng Rui(郑 锐)[c)], and Duan Chuan-Xi(段传喜)[a)†]

[a)] College of Physical Science and Technology, Central China Normal University, Wuhan 430079, China
[b)] College of Physical Science and Technology, Yangtze University, Jingzhou 434023, China
[c)] School of Mathematics & Information Science, North China University of Water Resources and Electric Power, Zhengzhou 450011, China

(Received 16 April 2014; revised manuscript received 15 July 2014; published online 10 October 2014)

The rovibrational spectrum of O_2–N_2O van der Waals complex is measured in the ν_1 symmetric stretch region of N_2O monomer using a tunable diode laser spectrometer. The complex is generated by a slit-pulsed supersonic expansion with gas mixtures of O_2, N_2O, and He. Both *a*- and *b*-type transitions are observed. The effective Hamiltonian for an open-shell complex consisting of a diatomic molecule in a $^3\Sigma$ electronic state and a closed-shell partner is used to analyze the observed spectrum. Molecular constants in the vibrationally excited state are determined accurately. The band-origin of the spectrum is determined to be 1284.7504(25) cm^{-1}, red-shifted from that of the N_2O monomer by ~ 0.1529 cm^{-1}.

Keywords: rovibrational spectrum, van der Waals complex, intermolecular interactions

PACS: 33.15.Mt, 33.20.Ea, 36.40.Mr **DOI:** 10.1088/1674-1056/23/12/123301

1. Introduction

High resolution spectroscopy of open-shell van der Waals complex consisting of an open-shell molecule and a closed-shell partner is an important method to study the intermolecular interactions involving open-shell molecules' interaction. Because of the nonzero electron spin introduced by the presence of one or more unpaired electrons, the spectra of open-shell molecules and complexes are relatively complicated and their analyses remain a great challenge.[1–4] Despite the importance of molecular oxygen in many fields, intermolecular interactions, specifically the interactions between oxygen and other molecules, are not well understood. For example, the available spectroscopic data for oxygen-containing complexes are limited to Ne–O_2,[5] Ar–O_2,[6,7] O_2–H_2O,[8–11] O_2–SO_2,[12,13] O_2–N_2O,[14,15] O_2–HF, and O_2–DF.[16–18] These experimental studies have been accompanied by several theoretical studies.[5,8,19–25] Spectroscopic investigations of the O_2–N_2O complex are of atmospheric interest, because a precise characterization of the weak interaction between O_2 and N_2O is essential for the accurate calculation of the O_2 pressure-broadening coefficient of N_2O. The available experimental studies on O_2–N_2O are limited to the infrared region. The vibrational spectra of O_2–N_2O in the N_2O ν_1 and ν_3 regions were detected by matrix isolation technique when O_2 was added to a nitrogen matrix diluted with N_2O.[14] The rotationally resolved spectrum of O_2–N_2O in the N_2O monomer ν_3 asymmetric stretching region was measured with the supersonic expansion method.[15] Spectroscopic data of Ref. [15] was refitted by W. M. Fawzy with a different effective Hamiltonian and the two results are almost the same.[26]

In this paper, we present the rovibrational spectrum of O_2–N_2O in the ν_1 symmetric stretching region of N_2O monomer. Accurate molecular constants in the vibrationally excited state are deduced from a nonlinear least-square fitting of observed transition frequencies. The results are compared with those obtained in the N_2O ν_3 region.

2. Experimental details

The tunable mid-infrared diode laser spectrometer used to record the absorption spectra of van der Waals complexes has been described in detail previously.[27,28] Briefly, the infrared radiation source is a lead-salt diode laser which is mounted in a liquid-nitrogen cooled Dewar (L5736, Laser Components). The laser beam enters into a vacuum chamber through a CaF_2 window after collimation. The laser controller (L5830, Laser Components) is used to modulate the current of a diode laser by a ramp waveform at a frequency of 1 kHz. The laser beam is reflected 120 times by two astigmatic mirrors in the chamber, and is arranged in the direction almost perpendicular to the jet expansion to minimize Doppler broadening. The chamber is evacuated by a 1500-L/s turbo-molecular pump backed with a 15-L/s mechanical pump. The background pressure is less than 2×10^{-6} mbar (1 bar = 10^5 Pa). A small portion of the laser beam is reflected by a CaF_2 beam splitter before it enters into the chamber, and is sent through a reference gas cell and an internally coupled confocal Fabry–Perot

*Project supported by the National Natural Science Foundation of China (Grants Nos. 11174098, 11304023, and 11304095).
†Corresponding author. E-mail: cxduan@phy.ccnu.edu.cn
© 2014 Chinese Physical Society and IOP Publishing Ltd

interferometer (IC-FPI) alternatively.[29] The spectra are calibrated against accurate frequencies of N_2O absorption lines taken from the HITRAN database[30] and the IC-FPI fringes (FSR~ 0.01 cm^{-1}). The absolute accuracy of frequency calibration is estimated to be about 5×10^{-4} cm^{-1}. Direct absorption signals of the jet, reference gas or interferometer fringes are detected by two liquid-nitrogen cooled HgCdTe detectors (Judson Technologies) separately. A 14-bit 50-MHz A/D card (NI PXI-5122) is used for data acquisition.

The O_2–N_2O complex is generated in a pulsed supersonic expansion through a 50 mm×200 μm slit nozzle which is attached to two 0.8-mm pinhole pulsed valves (General Valve series 9). The two pulsed valves are driven by two pulse controllers (IOTA ONE) synchronously with an opening duration of 1.5 ms and a repetition rate of 3 Hz. The sample gas is a mixture of N_2O ($\sim 0.5\%$), O_2 ($\sim 5\%$), and He. The optimal stagnation pressure is about 10 bar. Each spectrum is averaged over more than 3000 pulses.

3. Theoretical background

The theory for the rotational energy levels of O_2–N_2O has been described in detail previously.[15,31] Here only a brief description is given. The structure of the O_2–N_2O complex is assumed to be planar and can be described by the body-fixed coordinate X, Y, Z axes of the complex and x, y, z axes of O_2 molecule in the I^r representation. The Z and z axes are chosen such that they are coincident with the complex principle a axis and the O_2 internuclear axis respectively, while Y and y axes are both perpendicular to the complex plane. The relative positions of two monomers are defined by the intermolecular distance between O_2 and N_2O centers of mass (R), the angles of O_2 and N_2O's internuclear axis with respect to complex principle a axis (θ_1 and θ_2) respectively, and the azimuthal angle between O_2 z axis and complex plane (φ). The angle θ_1 is defined as θ in Refs. [15] and [31].

When an open-shell species is bounded with a closed-shell partner, the electronic spin–spin interaction is non-negligible due to the nonzero electron spin introduced by the unpaired electron(s). In order to analyze the infrared spectrum of O_2–N_2O open-shell complex in the ν_1 band region of N_2O, an effective Hamiltonian model consisting of rotational, centrifugal distortion and electron spin–spin interaction terms has been developed.[31] The effective Hamiltonian can be expressed as

$$\begin{aligned} H_{\rm eff} &= A(J_a-S_a)^2+B(J_b-S_b)^2+C(J_c-S_c)^2 \\ &\quad -D_J(\boldsymbol{J}-\boldsymbol{S})^4-D_{JK}(\boldsymbol{J}-\boldsymbol{S})^2(J_a-S_a)^2 \\ &\quad -D_K(J_a-S_a)^4+d_1(\boldsymbol{J}-\boldsymbol{S})^2 \\ &\quad \times[(J_+-S_+)^2+(J_--S_-)^2]+\frac{2\lambda}{3}(3S_z^2-\boldsymbol{S}^2), \quad (1) \end{aligned}$$

where A, B, and C are the rotational constants; D_J, D_{JK}, D_K, and d_1 are the centrifugal distortion constants; λ is the effective spin–spin coupling constant of the complex; S_a, S_b, and S_c are the projections of spin angular momentum along principle a, b, and c axes of the complex respectively; S_z is the projection of spin angular momentum along the z axis in the O_2 body-fixed coordinate; $J_\pm = J_b \mp \mathrm{i}J_c$ and $S_\pm = S_x \pm \mathrm{i}S_y$ are the raising (+) and lowering (−) operators, respectively.

The energy levels of the complex with parity $(-1)^{J-K_a-S+\Sigma+1}$ are denoted as e levels and those with $-(-1)^{J-K_a-S+\Sigma+1}$ are marked as f levels, where K_a is the projection of J along the a axis and Σ is the projection of electron spin S along the O_2 internuclear axis.

4. Results

The absorption spectra of the supersonic jet with gas mixtures of O_2/N_2O/He are measured in the N_2O ν_1 band region from 1284 cm^{-1} to 1285.6 cm^{-1}. A portion of the observed spectrum is deposited in Fig. 1(a). Strong absorption lines of N_2O monomer in the jet are removed for clarity.

The observed spectrum is very dense and probably contributed by several complexes or clusters formed in the jet. Therefore, the first step is to rule out those lines belonging to known species. The absorption spectrum in a supersonic expansion with $\sim 0.5\%$ of N_2O diluted in helium is also measured for comparison. A portion of the observed spectrum is shown in Fig. 1(b). Close inspection of the two spectra in Figs. 1(a) and 1(b) indicates that many absorption lines of $(N_2O)_2$[32] and $(N_2O)_3$[33] clusters are observed under both experimental conditions. Those additional lines that are observed only after O_2 has been added to the gas mixtures of N_2O/He are then ascribed to the O_2–N_2O complex.

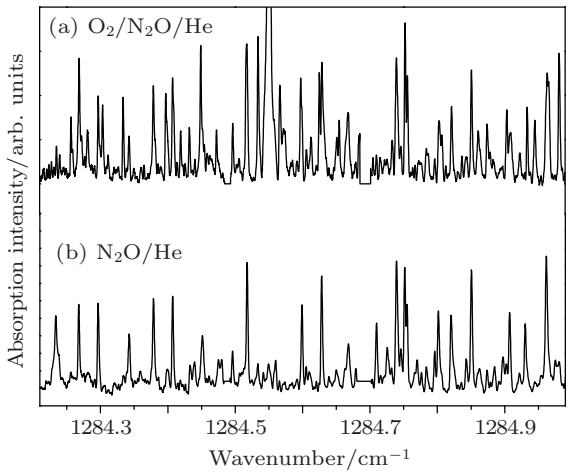


Fig. 1. Part of the absorption spectra observed in the supersonic expansion with gas mixtures of (a) O_2/N_2O/He and (b) N_2O/He. The N_2O monomer lines are removed for clarity.

Table 1. Observed transition frequencies (in cm^{-1}) of O_2–N_2O complex in the ν_1 stretch region of N_2O monomer.

Subband	J'	K'_a	e/f	J''	K''_a	e/f	Obs. Freq.[a]
$^{Q}P_0(J)$	4	0	e	5	0	e	1284.1149(–2)
	2	0	e	3	0	e	1284.3648(3)
$^{Q}R_0(J)$	3	0	e	2	0	e	1285.1333(–6)
	6	0	e	5	0	e	1285.5047(–1)
$^{Q}P_1(J)$	4	1	e	5	1	e	1284.1343(–1)
	3	1	e	4	1	e	1284.1986(–3)
	1	1	e	2	1	e	1284.5023(2)
$^{Q}R_1(J)$	2	1	e	1	1	e	1285.0231(–5)
	3	1	e	2	1	e	1285.1607(0)
	4	1	e	3	1	e	1285.2978(4)
	5	1	e	4	1	e	1285.3617(3)
	6	1	e	5	1	e	1285.4836(3)
$^{Q}R_2(J)$	5	2	f	4	2	f	1285.4053(–3)
	5	2	f	4	2	f	1285.4206(–1)
$^{R}Q_0(J)$	1	1	f	1	0	e	1284.9637(5)
	2	1	f	2	0	e	1284.9810(0)
	3	1	f	3	0	e	1285.0090(1)
	4	1	f	4	0	e	1285.0477(0)
	5	1	f	5	0	e	1285.0989(0)
	6	1	f	6	0	e	1285.1635(5)
	7	1	f	7	0	e	1285.2403(0)
$^{P}Q_1(J)$	1	0	e	1	1	f	1284.5340(–2)
	2	0	e	2	1	f	1284.5164(0)
	4	0	e	4	1	f	1284.4492(–3)
	5	0	e	5	1	f	1284.3972(–9)
	6	0	e	6	1	f	1284.3337(0)
	7	0	e	7	1	f	1284.2552(–9)
	8	0	e	8	1	f	1284.1666(9)
$^{R}R_0(J)$	1	1	e	0	0	e	1285.0786(10)
	2	1	e	1	0	e	1285.1939(–6)
	4	1	e	3	0	e	1285.4131(10)
	5	1	e	4	0	e	1285.5147(–6)
$^{P}P_1(J)$	0	0	e	1	1	e	1284.4193(–5)
	1	0	e	2	1	e	1284.3031(2)
	2	0	e	3	1	e	1284.1919(3)
	3	0	e	4	1	e	1284.0847(–3)
$^{R}P_0(J)$	4	1	e	5	0	e	1284.2676(–4)
	5	1	e	6	0	e	1284.1247(–6)
$^{P}R_1(J)$	2	0	e	1	1	e	1284.8066(1)
	3	0	e	2	1	e	1284.9451(0)
	4	0	e	3	1	e	1285.0865(0)
	5	0	e	4	1	e	1285.2286(–4)
	6	0	e	5	1	e	1285.3719(6)
$^{R}Q_1(J)$	6	2	e	6	1	f	1285.3163(–2)
	3	2	e	3	1	f	1285.3419(–2)
	2	2	e	2	1	f	1285.3546(6)
	2	2	f	2	1	e	1285.3971(–1)
	3	2	f	3	1	e	1285.4251(–5)
	4	2	f	4	1	e	1285.4637(1)
	6	2	f	6	1	e	1285.5665(–3)
$^{P}Q_2(J)$	2	1	e	2	2	f	1284.1388(–4)
	3	1	e	3	2	f	1284.1512(2)
	4	1	e	4	2	f	1284.1630(2)
	5	1	e	5	2	f	1284.1727(7)
	6	1	e	6	2	f	1284.1770(9)
	7	1	e	7	2	f	1284.1727(–2)
	8	1	e	8	2	f	1284.1615(5)
	9	1	e	9	2	f	1284.1388(–4)
	10	1	e	10	2	f	1284.1064(–4)
$^{R}P_1(J)$	7	2	f	8	1	e	1284.1461(7)
	6	2	f	7	1	e	1284.3113(6)
	5	2	f	6	1	e	1284.4725(–7)
$^{P}R_2(J)$	6	1	f	5	2	f	1285.0193(–1)
	7	1	f	6	2	f	1285.1808(–7)

[a]Number in each parenthesis is (obs.–cal.) frequency in units of the last digit.

The assignment and fitting of the transitions for the O_2–N_2O complex are performed with the aid of Fawzy's program[34] and molecular constants of O_2–N_2O reported in Ref. [15]. A total of 64 lines are assigned to the O_2–N_2O complex, including 14 a-type and 50 b-type transitions. All the transitions are within the $\Sigma = 0$ subgroup of levels. The observed transition frequencies and their assignments and residuals are listed in Table 1. Transitions are marked with quantum number J, K_a, and parity of rotational energy levels. The subbands are marked by $^{\Delta K_a}\Delta J_{K''_a}(J'')$. In the final fitting, centrifugal distortion constants are fixed at zero because their uncertainties are very large if floated. The angle between the complex a axis and O_2 z axis (θ_1) and the effective spin–spin coupling constant (λ) in the excited state are constrained to be the same as in the ground state. The fitting results are listed in Table 2. The standard deviation of the fitting is 4.89×10^{-4} cm^{-1}, which is within the experimental uncertainty. As can be seen in Table 2, molecular constants in the ground state determined in this work are in good agreement with those derived in Ref. [15]. The latter are with better accuracy. It may be due to the fact that the spectrum of O_2–N_2O[15] observed in the ν_3 region of N_2O is nearly free of interferences from the clusters of N_2O.

Table 2. Molecular constants of O_2–N_2O complex. In the table, the number in each parenthesis is one standard deviation of the fitting. All parameters except the angle θ_1 (in degrees), are in units of cm^{-1}.

Parameter	N_2O ν_3-excited[15]	N_2O ν_1-excited
ν_0	2224.12300(23)	1284.7504(25)
A''	0.36111(59)	0.3627(14)
B''	0.075725(25)	0.075744(55)
C''	0.062705(30)	0.062755(22)
A'	0.35671(49)	0.36085(19)
B'	0.075775(27)	0.075739(19)
C'	0.062609(19)	0.062739(18)
λ	1.6741(53)	1.6498(32)
θ_1	53.11(12)	53.15(42)
σ	0.000476	0.000489

A simulated spectrum of O_2–N_2O with molecular constants listed in Table 2 is shown in Fig. 2(b) for comparison with the observed spectrum. A rotational temperature of 5 K and a Doppler line width of 0.002 cm^{-1} are assumed in the simulation. It should be pointed out that a strong feature at $\sim$ 1284.550 cm^{-1}, which is asterisked in Fig. 2(a), cannot be assigned to any of the known bands of the N_2O monomer or its complexes. This feature is not observed in the He/N_2O expansion. The carrier of this strong feature is still unknown.

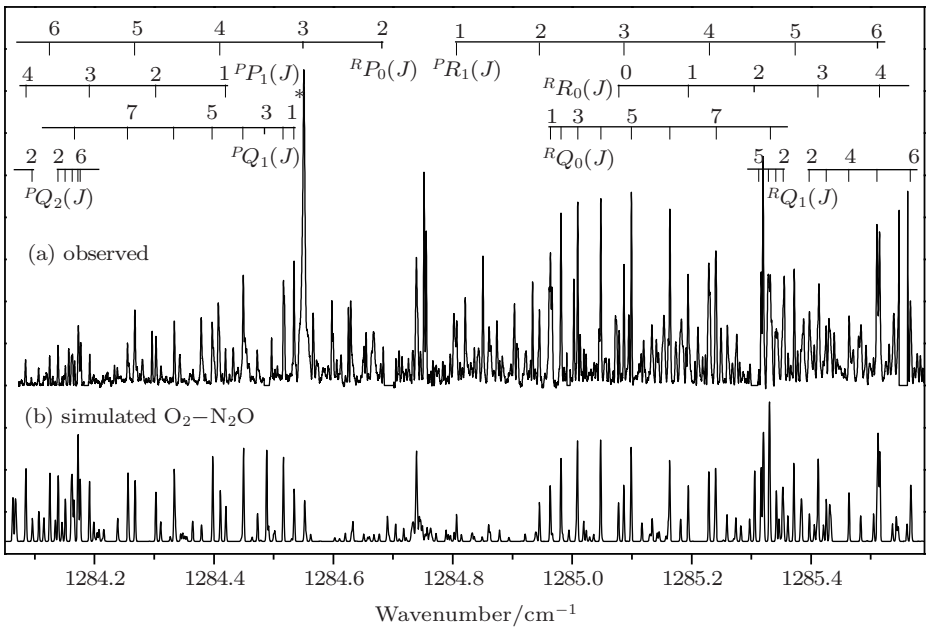


Fig. 2. (a) An overall view of the absorption spectrum observed in the slit jet expansion of O_2/N_2O/He gas mixtures. Assigned transitions of O_2–N_2O are marked. The N_2O monomer lines are removed for clarity. The strong feature marked with an asterisk is not assigned. (b) The simulated spectrum of O_2–N_2O.

5. Discussion

The rotational constants derived from the least-squares fitting indicate that O_2–N_2O complex is a near prolate top with $\kappa \approx -0.9$. Compared with the value in the ground state, the values of rotational constant A in the v_1 and v_3 vibrationally excited states are reduced by $\sim 0.51\%$ and $\sim 1.22\%$, respectively. It can be understood by the fact that the N_2O subunit in the complex is slightly expanded in the direction nearly parallel to the b-axis in both the v_1 and v_3 stretching modes of N_2O.

The band origin of the complex in the N_2O v_1 stretch region is 1284.7504(25) cm^{-1}. It is red-shifted by about 0.1529 cm^{-1} from that of the N_2O monomer, indicating a stronger intermolecular interaction and an increased potential well depth in the excited state. In contrast, the band origin in the v_3 band region is found to be blue-shifted by about 0.3663 cm^{-1}.[15] The band origin shift (Δv_0) of O_2–N_2O is also much smaller than those of N_2–N_2O, i.e., +0.83634 cm^{-1} [27] and +2.2327 cm^{-1} [35] upon v_1 and v_3 vibrational excitation respectively, as listed in Table 3. The unusual behavior of the band-origin shift for O_2–N_2O may arise from the characteristics of its open-shell structure.

Table 3. Structural parameters of O_2–N_2O and N_2–N_2O complexes in different vibrational states.

Parameter	O_2–N_2O			N_2–N_2O		
	Ground[a]	v_1[b]	v_3[a]	Ground[c]	v_1[c]	v_3[d]
Δv_0/cm^{-1}		–0.1529	+0.3663		+0.83634	+2.2327
Δ/amu·Å^2	–0.53(10)	–0.60(10)	–0.61(13)	1.98(8)	2.02(9)	1.99(12)
R_{cm}/Å	3.4232(10)	3.4202(4)	3.4243(6)	3.6926(3)	3.6929(3)	3.6954(4)

[a]Ref. [15], [b]this work. [c]Ref. [27]. [d]Ref. [35].

The inertial defect ($\Delta = I_c - I_a - I_b$) for O_2–N_2O complex can be deduced from corresponding rotational constants. The inertial defects in the ground and v_3 excited states are $-0.53(10)$ amu·Å^2 and $-0.61(13)$ amu·Å^2 respectively.[15] The inertial defect in the v_1 excited state, determined from this study, is $-0.60(10)$ amu·Å^2. The small negative value of the inertial defect indicates that the O_2–N_2O complex may not be planar, or large-amplitude out of plane motion is present in the complex. In contrast, the inertial defects for the closed-shell N_2–N_2O complex are 1.98(8) amu·Å^2 in the ground state,[27] 2.02(9) amu·Å^2 in the v_1 excited state,[27] and 1.99(12) amu·Å^2 in the v_3 excited state[35] as listed in Table 3. These small positive values of the inertial defect indicate that N_2–N_2O has a planar geometry in both the ground and vibrationally excited states.

The variation of intermolecular distance upon vibrational

excitation can be extracted from the relevant rotational constants. Assuming that the complex is planar, the following formula can be used to calculate the intermolecular distance between the mass centers of O_2 and N_2O:

$$R_{\rm cm} = \left[\frac{k}{\mu}\left(\frac{1}{C} - \frac{1}{b_{\rm N_2O}} - \frac{1}{b_{\rm O_2}}\right)\right]^{1/2}, \qquad (2)$$

where k is a conversion factor (16.8576 $\rm cm^{-1}\cdot amu\cdot Å^2$), μ is the reduced mass of the complex, C is the rotational constant of the complex, $b_{\rm N_2O}$ and $b_{\rm O_2}$ are rotational constants for two subunits respectively.[15,27] The values of $R_{\rm cm}$ of O_2–N_2O are 3.4232(10) Å in the ground state, 3.4202(4) Å and 3.4243(6) Å in the v_1 and v_3 excited states, respectively. The relative change of $R_{\rm cm}$ upon the vibrational excitation of the v_1 and v_3 stretching modes of O_2–N_2O is consistent with the relative shift of the corresponding band-origins. The intermolecular distance in N_2–N_2O is $\sim$ 3.69 Å as listed in Table 3, which is about 0.27 Å longer than that in O_2–N_2O. A shorter intermolecular distance usually implies a stronger intermolecular interaction. However, the calculated global minimum energy of O_2–N_2O is -191 $\rm cm^{-1}$,[15] while it is -326.64 $\rm cm^{-1}$ for N_2–N_2O.[27] The unusual characteristics of O_2–N_2O might arise from the non-zero electron spin in the O_2 subunit.

6. Conclusion

In this work, the high-resolution spectrum of the O_2–N_2O open-shell complex is measured by a mid-infrared tunable diode laser spectrometer in the N_2O monomer v_1 symmetric stretch region. The observed transition frequencies are fitted successfully with a standard effective Hamiltonian for open-shell van der Waals complex, yielding accurate molecular constants of the complex in the vibrationally excited state. The comparisons of molecular constant and structural parameter between the O_2–N_2O complex and the N_2–N_2O complex indicate that the open-shell complex has some unusual characteristics.

References

[1] Wu L, Zheng L J, Kaniki K, Chen Y Q and Yang X H 2007 *Chin. Phys. Lett.* **24** 90
[2] Zhu Z L, Lang J H and Qiao H 2013 *Acta Phys. Sin.* **62** 163103 (in Chinese)
[3] Gao X Y, You K, Zhang X M, Liu Y L and Liu Y F 2013 *Acta Phys. Sin.* **62** 233302 (in Chinese)
[4] Shao X P, Zhao M and Yang X H 2013 *Chin. Phys. B* **22** 073302
[5] Beneventi L, Casavecchia P, Pirani F, Vecchiocattivi F, Volpi G, Brocks G, van der Avoird A, Heijmen B and Reuss J 1991 *J. Chem. Phys.* **95** 195
[6] Henderson G and Ewing G E 1973 *J. Chem. Phys.* **59** 2280
[7] Mettes J, Heyrnen B, Verhoeve P, Reuss J, Laine D C and Brocks G 1985 *Chem. Phys.* **92** 9
[8] Gomes J A G, Gossage J L, Balu H, Kesmez M, Bowen F, Lumpkin R S and Cocke D L 2005 *Spectrochimica Acta Part A* **61** 3082
[9] Cooper P D, Kjaergaard H G, Langford V S, McKinley A J, Quickenden T I, Robinson T W and Schofield D P 2005 *J. Phys. Chem. A* **109** 4274
[10] Kuma S, Slipchenko M N, Momose T and Vilesov A F 2010 *J. Phys. Chem. A* **114** 9022.
[11] Kasai Y, Dupuy E, Saito R, Hashimoto K, Sabu A, Kondo S, Sumiyoshi Y and Endo Y 2011 *Atmos. Chem. Phys.* **11** 8607
[12] Walker A R H, Fraser G T, Hougen J T, Lugez C L, Suenram R D and Fawzy W M, "Electron-spin and tunneling effects in the microwave spectrum of SO_2–O_2", in: WI-08, the 52*nd International Symposium on Molecular Spectroscopy*, 1997, Ohio State University, Columbus, Ohio, USA
[13] Walker A R H, Fraser G T, Hougen J T, Suenram R D, Fawzy W M and Novick S E, "An improved fit of the microwave spectrum of SO_2–O_2", in: FD-08, the 53*rd International Symposium on Molecular Spectroscopy*, 1998, Ohio State University, Columbus, Ohio, USA
[14] Bahou M, Schriver-Mazzuoli L, Camy-Peyret C, Schriver A, Chiavassa T and Aycard J P 1997 *Chem. Phys. Lett.* **265** 145
[15] Qian H B, Seccombe D and Howard B J 1997 *J. Chem. Phys.* **107** 7658
[16] Hunt R D and Andrews L 1987 *J. Chem. Phys.* **86** 3781
[17] Fawzy W M, Lovejoy C M, Nesbitt D J and Hougen J 2002 *J. Chem. Phys.* **117** 693
[18] Wu S, Sedo G, Grumstrup E M and Leopold K R 2007 *J. Chem. Phys.* **127** 204315
[19] van Lenthe J H and van Duijneveldt F B 1984 *J. Chem. Phys.* **81** 3168
[20] Cybulski S M, Kendall R A, Chalasinski G, Severson M W and Szczesniak M M 1997 *J. Chem. Phys.* **106** 7731
[21] Sabu A, Kondo S, Miura N and Hashimoto K 2004 *Chem. Phys. Lett.* **391** 101
[22] Sabu A, Kondo S, Saito R, Kasai Y and Hashimoto K 2005 *J. Phys. Chem. A* **109** 1836
[23] Sapse A M 1983 *J. Chem. Phys.* **78** 5733
[24] Reed A E, Weinhold F, Curtiss L A and Pochatko D J 1984 *J. Chem. Phys.* **84** 5687
[25] Fawzy W M 2006 *J. Chem. Phys.* **124** 164303
[26] Fawzy W M 1998 *J. Chem. Phys.* **109** 348
[27] Zheng R, Zhu Y, Li S, Fang M and Duan C X 2011 *J. Mol. Spectrosc.* **265** 102
[28] Li S, Zheng R, Zhu Y and Duan C X 2011 *J. Chem. Phys.* **134** 134304
[29] Reich M, Schieder R, Clar H J and Winnewisser G 1986 *Appl. Opt.* **25** 130
[30] L S Rothman et al. 2009 *Journal of Quantitative Spectroscopy and Radiative Transfer* **110** 533
[31] Qian H B, Low S J, Seccombe D and Howard B J 1997 *J. Chem. Phys.* **107** 7651
[32] Dehghany M, Afshari M, Thompson R I, Moazzen-Ahmadi N and McKellar A R W 2008 *J. Mol. Spectrosc.* **252** 1
[33] Dehghany M, Afshari M, Moazzen-Ahmadi N and McKellar A R W 2009 *J. Chem. Phys.* **130** 044303
[34] Fawzy W M 2010 *Comp. Phys. Comm.* **181** 1789
[35] Randall R W, Dyke T R and Howard B J 1988 *Faraday. Discuss. Chem. Soc.* **86** 21